

# Molecular Cloning, Chromosomal Localization, Tissue mRNA Levels, Bacterial Expression, and Enzymatic Properties of Human NMN Adenylyltransferase\*

Received for publication, September 22, 2000, and in revised form, October 4, 2000  
Published, JBC Papers in Press, October 10, 2000, DOI 10.1074/jbc.M008700200

Monica Emanuelli‡, Francesco Carnevali‡, Franca Saccucci§, Francesca Pierella‡, Adolfo Amici‡, Nadia Raffaelli‡, and Giulio Magni‡¶

From the Istituti di ‡Biochimica e §Biologia e Genetica, Facoltà di Medicina e Chirurgia, University of Ancona, via Ranieri, 60100 Ancona, Italy

**A 1329-base pair clone isolated from a human placenta cDNA library contains a full-length 837-base pair coding region for a 31.9-kDa protein whose deduced primary structure exhibits high homology to consensus sequences found in other NMN adenylyltransferases. Northern blotting detected a major 3.1-kilobase mRNA transcript as well as a minor 4.1-kilobase transcript in all human tissues examined. In several cancer cell lines, lower levels of mRNA expression were clearly evident. The gene encoding the human enzyme was mapped to chromosome band 1p32–35. High efficiency bacterial expression yielded 1.5 mg of recombinant enzyme/liter of culture medium. The molecular and kinetic properties of recombinant human NMN adenylyltransferase provide new directions for investigating metabolic pathways involving this enzyme.**

Following genomic damage by various chemical or radiation treatments, the extent of malignant transformation is thought to be limited by enhanced DNA repair. Such repair is accomplished by activation of different metabolic processes, some involving NAD<sup>+</sup>. This indicates that the pyridine coenzyme NAD<sup>+</sup> plays significant roles beyond its participation in redox metabolism and in various types of ADP-ribosylation. The cellular NAD<sup>+</sup> concentration likewise appears to modulate expression of stress response proteins, including the tumor suppressor protein p53. In fact, high levels of pyridine dinucleotide reduce the time required for cellular rescue from DNA damage. Skin biopsy specimens from actinic keratoses and squamous cell carcinomas also exhibit an inverse relationship between skin NAD<sup>+</sup> content and the severity of the malignant phenotype (1). In view of this role of NAD<sup>+</sup> in cellular rescue from DNA damage, a better understanding of how human NAD<sup>+</sup> biosynthesis is regulated may be of vital importance in developing effective approaches for preventing and treating cancer.

For many years, we have studied NMN adenylyltransferases (NMNATs),<sup>1</sup> which play central roles in both *de novo* biosyn-

thetic and salvage pathways for nicotinamide nucleotides. These enzymes convert NMN (or nicotinic acid mononucleotide) and ATP to NAD<sup>+</sup> (or nicotinic acid adenine dinucleotide) and inorganic pyrophosphate (2), and their activity has been correlated with crucial cellular events such as mitosis and DNA synthesis (3, 4). In prokaryotes, cell survival and viability appear to require NMNAT activity (5). Because tumor cell NMNAT concentrations are very low, the enzyme represents a potential chemotherapeutic target (6, 7). This adenylyltransferase catalyzes the essential last step in the metabolic conversion of the potent antitumor agent tiazofurin from its prodrug form to tiazofurin adenine dinucleotide. Low tumor levels of this enzyme activity are associated with the development of drug resistance (8, 9).

Our laboratory has purified and characterized NMN adenylyltransferases from yeast, bull testis, thermophilic bacteria, and human placenta (10–13). We have also identified, cloned, and expressed the gene for this enzyme from *Methanococcus jannaschii* and *Saccharomyces cerevisiae* (12, 14), as well as from *Synechocystis* sp. (*slr0787*). The bifunctional *slr0787* protein is endowed with both nudix hydrolase and NMNAT activities; and in *Escherichia coli*, the NAD<sup>+</sup> biosynthesis regulatory protein NadR possesses NMNAT activity (15, 16). As part of an ongoing study on the role of this enzyme in regulating NAD<sup>+</sup> levels, we successfully isolated a full-length cDNA encoding NMNAT from a human placenta cDNA library. In this report, we describe human NMNAT cDNA cloning and its tissue-specific expression, levels in tumor cells, and chromosomal location. We also describe the high efficiency expression and purification of the protein in *E. coli* as well as its kinetic properties and metal ion effects.

## EXPERIMENTAL PROCEDURES

### Materials

We purchased a human placenta cDNA library constructed in  $\lambda$ gt11 as well as blots containing poly(A)<sup>+</sup> RNAs from human tissues and cancer cell lines from CLONTECH (Palo Alto, CA). Restriction endonucleases and other cloning reagents were purchased from New England Biolabs, Inc. (Beverly, MA) or Promega (Madison, WI). Double-stranded DNA probes were radiolabeled with [ $\alpha$ -<sup>32</sup>P]dCTP (3000 Ci/mmol) from Amersham Pharmacia Biotech (Buckinghamshire, United Kingdom) using a commercial random priming kit (Amersham Pharmacia Biotech, Uppsala, Sweden). All other reagent-grade chemicals were obtained from standard suppliers.

### Methods

Human placental NMNAT was purified (13) and subjected to tryptic digestion (17). The resulting fragments were separated by reverse-

\* This work was supported in part by Consiglio Nazionale delle Ricerche Target Project "Biotechnology" and by Cofinanziamento Ministero dell'Università e della Ricerca Scientifica e Tecnologica "Nucleotidi e Nucleosidi: Segnali Chimici, Regolatori Metabolici e Potenziali Farmaci." The costs of publication of this article were defrayed in part by the payment of page charges. This article must therefore be hereby marked "advertisement" in accordance with 18 U.S.C. Section 1734 solely to indicate this fact.

The nucleotide sequence(s) reported in this paper has been submitted to the GenBank™/EBI Data Bank with accession number(s) AF312734.

¶ To whom correspondence should be addressed. Tel.: 390-71-2204678; Fax: 390-71-2802117; E-mail: magni@popcsi.unian.it.

<sup>1</sup> The abbreviations used are: NMNAT, NMN adenylyltransferase;

bp, base pair; PCR, polymerase chain reaction; HPLC, high performance liquid chromatography; BisTris, 2-[bis(2-hydroxyethyl)amino]-2-(hydroxymethyl)propane-1,3-diol.

phase liquid chromatography on an ABI 173A Capillary LC/Microblotter system. After spotting recombinant human NMNAT on a polyvinylidene difluoride membrane, Edman sequencing was performed on an Applied Biosystems Procise Model 491 sequencer.

**Identification and Isolation of Full-length cDNA for Human NMNAT**—BLAST searches (18), conducted with NMNAT peptides (YLVPDLVQEYIEK and NAGVILAPLQR) as query sequences, revealed a full match with the predicted amino acid sequence of an expressed sequence tag cDNA (GenBank™/EBI accession number AA307717). This clone, containing a 342-bp cDNA insert, was used to design PCR primers for the cloning of human NMNAT cDNA. We first employed PCR using a human placenta cDNA 5'-stretch  $\lambda$ gt11 library and primers based on the expressed sequence tag sequence (HATF, 5'-TACTTGGTACCAGATCTTGTCC-3'; and HATR, 5'-CTTCTGCAGTGTTTCTCTGCAA-3'). PCR was carried out in a GeneAmp PCR system 2400 (PerkinElmer Life Sciences) for 35 cycles of denaturation (95 °C, 30 s annealing (60 °C, 1 min), and extension (72 °C, 1 min). The resulting 118-bp fragment was sequenced to confirm the presence of NMNAT cDNA (see Fig. 1, sequence B, nucleotides 800–917).

The 5'-part of the human NMNAT cDNA was isolated by two consecutive PCRs. A primary PCR was performed with the  $\lambda$ gt11-specific primer V1 (5'-GAGCTCACACCAGACCACTGGTAATG-3') in combination with primer HATR directed upstream of sequence B (5'-CTTCTGCAGTGTTTCTCTGCAA-3'). To increase the specificity, the product of the first round of PCR was diluted 1:10 in water, and 1  $\mu$ l was used as a template in a second round of PCR using the nested  $\lambda$ gt11-specific primer V2 (5'-CAACTGGTAATGGTAGCG-3') and the nested specific primer HATR (5'-GGACAAGATCTGGTACCAAGTA-3'). This final combination yielded an 821-bp DNA fragment, which was cloned into the pGEM-T vector by T-A ligation for transformation of *E. coli* JM109 and sequenced on both strands (see Fig. 1, sequence A, nucleotides 1–821). Primers HATF and HATFN (5'-TTGCAGAGAAACACTGCAAG-3'), in combination with the  $\lambda$ gt11-specific primers V1 and V2, were used to isolate the 3'-part of the cDNA sequence. The product of the second round of PCR was a 434-bp fragment, which was cloned into the pGEM vector and sequenced (see Fig. 1, sequence C, nucleotides 896–1329).

**Construction of Expression Vector and Expression in *E. coli***—To prepare a vector suitable for expression of recombinant NMNAT in *E. coli*, we first generated an 840-bp DNA fragment containing the coding sequence for NMNAT by PCR of the aforementioned cDNA library using primers HF (5'-CGGGGATTTCATGGAAAATTCGAGAAGACT-3') and HR (5'-GCAGTCGACCTATGCTTAGCTTCTGCAGT-3'). Primer HF contains a *Bam*HI site followed by the beginning of the open reading frame; primer HR contains the end of the open reading frame followed by a *Sal*I cleavage site. PCR (1 min of denaturation at 95 °C, 1 min of annealing at 50 °C, and 1 min of elongation at 72 °C) was performed for 35 cycles with 20 pmol of each primer in a final volume of 100  $\mu$ l. After electrophoresis on a 1% agarose gel, the amplified DNA, visible by ethidium bromide staining, was digested with *Bam*HI and *Sal*I and cloned into *Bam*HI-*Sal*I-digested pT7-7 plasmid vector (19) to obtain the construct pT7-7-HAT. The insert was sequenced to ascertain that no mutations had been introduced during amplification. The construct was used to transform *E. coli* TOP10 (Invitrogen) for plasmid preparation and *E. coli* BL21(DE3) for protein expression.

**Growth and Expression of Recombinant Human NMNAT**—Transformed BL21(DE3) cells were grown at 37 °C to an  $A_{600}$  of 0.6 in LB medium (50 ml) containing 100  $\mu$ g/ml ampicillin. A 10-ml portion was used to inoculate 1 liter fresh LB medium containing 100  $\mu$ g/ml ampicillin, and the mixture was incubated overnight at 120 rpm at 37 °C. Protein production was then induced by 0.4 mM isopropyl- $\beta$ -D-thiogalactopyranoside. After a 3-h induction at 37 °C, cells were harvested by centrifugation (10,000  $\times g$  for 10 min at 4 °C) and either used for purification or stored at –80 °C.

**Purification of Recombinant Human NMNAT**—All steps were performed at 4 °C. The cell pellet was suspended in 60 ml of 100 mM Tris-HCl (pH 7.4) containing 0.5 mM EDTA, 1 mM  $MgCl_2$ , and 1 mM dithiothreitol (buffer A) and disrupted by sonication. The lysate was centrifuged at 15,000  $\times g$  for 30 min (crude extract). The crude extract was applied to a Matrex Gel Green A chromatography column, previously equilibrated with buffer A. The column was washed with the same buffer containing 0.5 M NaCl and eluted with a linear NaCl gradient (0.5–2.5 M) in the equilibration buffer (Green A fraction). After adding NaCl to a final concentration of 3 M, the Green A fraction was loaded onto a phenyl-Sepharose column, equilibrated with buffer A containing 3 M NaCl. The column was washed with buffer A containing 2 M NaCl and then eluted with a linear NaCl gradient (2 to 0 M in buffer A). The

active pool was concentrated through an Amicon YM-30 membrane (phenyl-Sepharose fraction). This fraction was injected onto a Superose 12 HR 10/30 fast protein liquid chromatography column (Amersham Pharmacia Biotech), previously equilibrated with 50 mM Tris-HCl (pH 7.4) containing 0.5 mM EDTA, 1 mM  $MgCl_2$ , 1 mM dithiothreitol, and 0.5 M NaCl. Active fractions were analyzed by SDS-polyacrylamide gel electrophoresis as described below. Homogeneous fractions were pooled and used to determine substrate specificity and other catalytic properties.

**Enzyme Activity Assays and Kinetic Characterization**—Enzyme activity was measured continuously by a coupled spectrophotometric assay (20) or by HPLC (20). Optimal reaction conditions were established by varying divalent cation concentration and buffer pH (30 mM BisTris-HCl and 30 mM Tris-HCl adjusted to the desired pH). One enzyme unit is defined as the amount that catalyzes formation of 1  $\mu$ mol of  $NAD^+$ /min at 37 °C.

**Chromosomal Mapping**—Human metaphase spreads were obtained from phytohemagglutinin-stimulated peripheral lymphocytes of a normal donor by standard procedures. Chromosome preparations were hybridized *in situ* with biotinylated probes (full-length human NMNAT cDNA) labeled by nick translation essentially as described by Lichter *et al.* (21). Labeled probe (500 ng) was used for fluorescence *in situ* hybridization at 37 °C in 2 $\times$  SSC, 50% formamide, 10% dextran sulfate, 5  $\mu$ g of COT1 DNA, and 3  $\mu$ g of sonicated salmon sperm DNA (10- $\mu$ l volume). Post-hybridization washing was carried out at 42 °C in 2 $\times$  SSC and 50% formamide (three times), followed by three washes in 0.1 $\times$  SSC at 60 °C. Biotin-labeled DNA was detected with Cy3-conjugated avidin. Chromosome identification was obtained by simultaneous 4,6-diamidino-2-phenylindole staining to produce the characteristic Q-banding patterns.

**Northern Blot Analysis**—Blots containing 2  $\mu$ g of poly(A)<sup>+</sup> RNA from different human tissues and cancer cell lines were prehybridized at 68 °C for 1 h in ExpressHyb™ hybridization solution. The filters were then hybridized with the <sup>32</sup>P-labeled cDNA probe (nucleotides 89–928) at 68 °C for 16 h. After washing as recommended by the manufacturer, blots were exposed to x-ray films at –80 °C with an intensifying screen for 4 days. RNA integrity and loading were assessed with an actin probe.

**Southern Blot Analysis**—Human genomic DNA (10  $\mu$ g) from human peripheral white blood cells was digested with *Apa*I, *Bam*HI, *Eco*RI, *Pst*I, or *Pvu*II. DNA fragments were resolved on a 1% agarose gel and transferred to a nylon membrane by the method of Southern (22). A 118-bp cDNA fragment (nucleotides 800–917) was amplified with primers HATF and HATR using the pT7-7-HAT construct as a template and gel-purified. This fragment, radiolabeled with [ $\alpha$ -<sup>32</sup>P]dCTP (3000 Ci/mmol) using the commercial random priming kit, was used as a probe. Hybridization was performed overnight at 45 °C in ULTRAhyb buffer (Ambion Inc.). The filter was then washed and exposed for 48 h to x-ray film at –80 °C.

Gel electrophoresis of recombinant human NMNAT was carried out by the Laemmli method (23) on 15% polyacrylamide gel. Gel filtration of recombinant human NMNAT was performed by fast protein liquid chromatography on a Superose 12 HR 10/30 column equilibrated with 50 mM Tris-HCl (pH 7.4) containing 0.5 M NaCl, 1 mM dithiothreitol, 1 mM  $MgCl_2$ , and 0.5 mM EDTA. Protein concentration was determined by the Bradford method (24).

## RESULTS AND DISCUSSION

**Isolation and Characterization of Human NMNAT cDNA**—Using two tryptic peptide sequences from human placental NMNAT, we conducted BLAST searches of the human expressed sequence tag data base. We identified a cDNA clone (GenBank™/EBI accession number AA307717) encoding both sequences. The insert of this clone was too short to account for the molecular mass of NMNAT (13), and we used the clone to design specific primers for PCR experiments utilizing a human placenta cDNA library. A scheme of our cloning strategy is shown in Fig. 1. The composite sequence obtained by assembling the products of PCR experiments resulted in a 1329-bp transcript consisting of an 88-bp 5'-untranslated region, an 837-bp coding region, and a 404-bp 3'-untranslated region with an incomplete AATAA polyadenylation signal (Fig. 2, upper panel). The translational initiation site (ATG), assigned to the first methionine codon (nucleotides 89–91), is in the favorable initiation context ACCATGG, thus fulfilling Kozak's criteria for



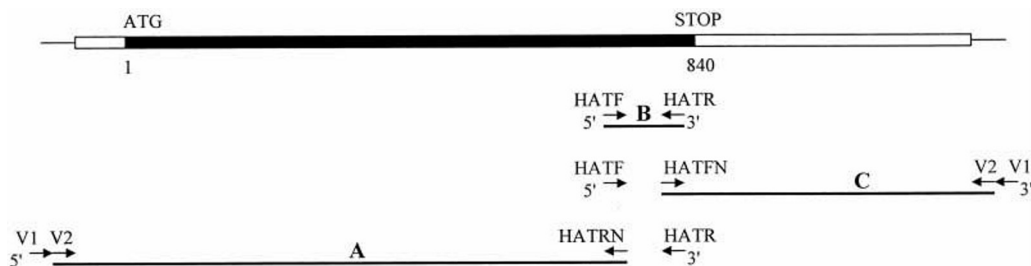
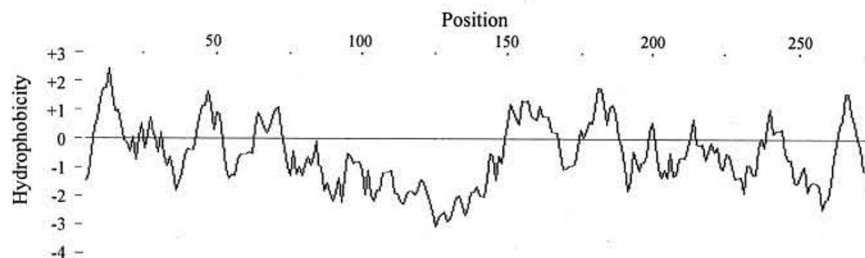


FIG. 1. Schematic representation of the cloning and sequencing strategy. The composite sequence of the human NMNAT cDNA is shown schematically at the top. Sequences A–C represent PCR-amplified fragments corresponding to different parts of the full-length sequence. The PCR primers and their positions in the full-length cDNA are indicated. See “Experimental Procedures” for details.

gcctcgccan	nngacgggca	gtgagggcag	ctgacaacag	gganggtgtc	acagttttcc	60
atttagatca	caacttcaag	ttcttaccat	ggaaaattcc	gagaagactg	aagtgggtct	120
			M E N S	E K T	E V V L	11
ccttgcttgt	gggtcattca	atcccatcac	caacatgcac	ctcaggttgt	ttgagctggc	180
L A C	G S F	N P I T	N M H	L R L	F E L A	31
caaggactac	atgaatggaa	caggaaggta	cacagttgtc	aaaggcatca	tctctcctgt	240
K D Y	M N* G	T G R Y	T V V	K G I	I S P V	51
tggtgatgcc	tacaagaaga	aaggactcat	tcctgcctat	caccgggtca	tcatggcaga	300
G D A	Y K K	K G L I	P A Y	H R V	I M A E	71
acttgctacc	aagaattcta	aatgggtgga	agttgatata	tgggaaagtc	ttcagaagga	360
L A T	K N S	K W V E	V D T	W E S	L Q K E	91
gtggaaagag	actctgaagg	tgctaagaca	ccatcaagag	aaattggagg	ctagtgtact	420
W K E	T L K	V L R H	H Q E	K L E	A S D C	111
tgatcaccag	cagaactcac	ccactctaga	aaggcctgga	aggaagagga	agtggactga	480
D H Q	Q N S	P T L E	R P G	R K R	K W T E	131
aacacaagat	tctagtcaaa	agaaatccct	agagccaaaa	acaaaagctg	tgccaaaggt	540
T Q D	S S Q	K K S L	E P K	T K A	V P K V	151
caagctgctg	tgtggggcag	atttattgga	gtcctttgct	gttcccaatt	tgtggaagag	600
K L L	C G A	D L L E	S F A	V P N	L W K S	171
tgaagacatc	accctaaatcg	tggccaacta	tgggctcata	tgtgttactc	gggctggaaa	660
E D I	T Q I	V A N Y	G L I	C V T	R A G N	191
tgtgctcag	aagtttatct	atgaatcgga	tgtgctgtgg	aaacaccgga	gcaacattca	720
D A Q	K F I	Y E S D	V L W	K H R	S N I H	211
cgtgggtgaat	gaatgggttcg	ctaattgacat	ctcatccaca	aaaatccgga	gagccctcag	780
V V N	E W F	A N D I	S S T	K I R	R A L R	231
aagggggccag	agcatttcgct	acttggttacc	agatcttgtc	caagaatata	ttgaaaagca	840
R G Q	S I R	Y L V P	D L V	Q E Y	I E K H	251
taattttgtac	agctctgaga	gtgaagacag	gaatgtctgg	gtcatcctgg	cccctttgca	900
N L Y	S S E	S E D R	N A G	V I L	A P L Q	271
gagaaacact	gcagaagcta	agacatagga	attctacagc	atgatatttc	agacttccca	960
R N T	A E A	K T	-			279
tttggggatc	tgaacaacac	tgggagttaa	taactgggga	aagaagtgtg	gacactgttg	1020
cctaaactaa	agctttaaag	tttagtataa	atcgtctggg	cacagtggct	cacgcctgta	1080
atcccagcac	tttggggaggc	tgaggcaggt	ggatcacggg	gtcaagagat	cgagaccatc	1140
ctggccaata	tgggtgaagcc	ccatctctac	taaaaataca	aaaattagct	gtgtgtgggt	1200
ggcacagtgc	ctgtagtccc	agctacttgg	gaggctgagg	caggagaatc	gcttgacccc	1260
aggtggtgga	gggtgcagtg	agccaagatt	gcaccattgc	actccagcct	gcacagagca	1320
agactctgt						1329

FIG. 2. Nucleotide and deduced amino acid sequences of cDNA encoding human NMNAT. In the upper panel, the numbers on the right refer to nucleotide and amino acid positions. The sequences determined for tryptic fragments of NMNAT from human placenta are underlined. The potential Asn-linked glycosylation site is marked with an asterisk. In the lower panel, the hydrophobicity profile for the translation of the cDNA sequence is shown. The analysis was performed according to Kyte and Doolittle (26). The hydrophobicity value of each amino acid residue is plotted against its position in the polypeptide ( $x$  axis), starting with the amino terminus.



initiation (25). An in-frame translational termination codon (TAG) occurs after nucleotide 925. The open reading frame encodes a 279-amino acid protein with a molecular mass of

31,900 Da, close to that estimated by SDS-polyacrylamide gel electrophoresis (13). When the sequences of both tryptic peptides were aligned with the deduced amino acid sequence, there

C. elegans - 1	-----MGTEKVVILAV	GSFNPETNG	20
C. elegans - 2	-----MKRVALLAV	GSFNPETIA	18
H. sapiens	-----MENSEKTEVLLAC	GSFNPITNM	23
S. cerevisiae	GVQKYQIADLEEVPHGIVRQARTLEDYEFPSHRLSKLLDPNKLPLVIVACGSFSPTITL		180
M. jannaschii	-----MRGFII	GRFQPHKG	15
Synechocystis	-----MQTKYQYGIYI	GRFQPHLG	20
E. coli (NadR)	QVADASGMTKGYLSQLLNAAIKSPSAQKLEALHRFLGLEFPQKKTIGVVF	GKFFPHTG	86
		* * *	
C. elegans - 1	HLCMMEDAKYSLEKSG-KIVLEGIMSPVSDGYAKK-SLISAKHRLAQTEAATY-DSDW--		75
C. elegans - 2	HLRMLEVARSHLETIN-TQVVEGIMSPVADSNNKPTLIKSNFRIQMVRATK-SSDW--		74
H. sapiens	HLRFLFELAKDYMGRTGRYTVVKGII SPVGDAYKK-GLIPAYHRVIMAEATK-NSKW--		79
S. cerevisiae	HLRMFEMALDAISEQTRFEVIGGYSPVSDNYQKQ-GLAPSYHRVIMCELACERTSSW--		237
M. jannaschii	HLEVIKKIAEEVD-----EIIIGIGSAQKSHTLEN--PFTAGERILMITQSLK-----		61
Synechocystis	HLRTLNLALEKAE-----QVIIILGSHRVAADTRN--PWRSPERMAMIEACLSPQILKRV		73
E. coli (NadR)	H		146
	*: ::	*	
C. elegans - 1	--IHASGWCAQSEWTATVNVLKHHQ--		100
C. elegans - 2	--IRADDWECTRTTWTRTIDVLRHHREL--		100
H. sapiens	--VEVDTWESLQKEWETLKVLRHHQEKLEASDCDHQONSPTLERPGRKRKWTETQDSSQ		137
S. cerevisiae	--LMVDAWESLQPSYTRTAKVLDHFNHEIN--	IKRG	269
M. jannaschii	----DYDLTYPIPIKDIEN		78
Synechocystis	HFLTVRDWLYSDNLWLAQVQQLKITGGS--	NSV	106
E. coli (NadR)	HAFNEEGMEPYPHGWDVWSNGIKFMAEKGIQPDLYTSEEADAPQYMEHLGIETVLVDP		206
C. elegans - 1	----DNKLGSDVNVLLFGGDVIESFDKFIADGTPVW--	DREDVE	139
C. elegans - 2	---VQEKFGSDVGMLLVGGDVVDSTFTRILPDGSNLW--	NSSDIR	140
H. sapiens	KKSLEPKTKAVPKVLLCGADLLESFAVFN--LW--	KSEDIT	175
S. cerevisiae	GVATVTGEKIGVKIMLLAGGDLIESMGEFN--VW--	ADADLH	307
M. jannaschii	-----S-----IW-VSYVESLTPFFD--		93
Synechocystis	VVLGHRKDASSYYLNLFPQWDYLETGHPDFSSSTAIRGAYFEGKEGDYLDKVPPIADYL		166
E. coli (NadR)	KRTFMSISGAQIRENPFYWEYIPTVEKPFVVRTVAILGGESSGKSTLVN--	KLANIF	262
		:::	
C. elegans - 1	EIISAG-I---VVRSRPGSDPEQTLKKLNLNENSDKVHFIKNAISSN-SISSTSLRAALK		194
C. elegans - 2	TIITEFGL---IVLSREGSNPLNTIQSMPAISFCDRIIQVKDEVCPSS-GVSSTSLRAAIM		196
H. sapiens	QIVANYGL---ICVTRAGNDAQKFIYESDVLWKHRSNIHVNEWNFAN-DISSTKIRRALR		231
S. cerevisiae	HILGNYGC---LIVERTGSDVRSFLLSHDIMYEHRRNIIKQLIYN-DISSTKVRLFIR		363
M. jannaschii	-----IVYS--GNPLVRVLFEERGVEVKRPEMFNRKEYSG-----TEIRRRML		134
Synechocystis	QTFQKSER---YIALCDEYQFLQAYKQAWATAPYAPTITDAVVVQ-AGHVLVVRROAK		222
E. coli (NadR)	NTTSAWEYGRDYVFSHLGGDEIALQYSDYDKIALGHAQYIDFAVKYANKVAFIDTDFVTT		322
C. elegans - 1	EHR-----SIKYTPDSVIKYIKDHRLYE-----		218
C. elegans - 2	NKK-----SIKYSTPDEVINFIRENNLYQKI-----		222
H. sapiens	RGQ-----SIRYLVDPDLVQEIYEKHNLYSSESDRNA		263
S. cerevisiae	RAM-----SVQYLLPNSVIRYIQEHRLVVDQTEPVKQ		395
M. jannaschii	NGE-----KWEHLVPAKAVVDVIKEIKGVERLRKLAQT		166
Synechocystis	PGLGLIALPGGFIQNETLVEGMLRELKEETRLKVLPLVLRGSIVDSHVFDAPGRSLRGR		282
E. coli (NadR)	QAFCK-----KYGREHPFVQALIDEYRFDLVILLENT		356

FIG. 3. Comparison of the amino acid sequence of human NMNAT with those of other homologous proteins. Shown is an optimized multiple sequence alignment created using the ClustalW program. Protein sequences included in the comparison are the translation of the human NMNAT cDNA (*Homo sapiens*), the two putative *C. elegans* homologs, the *S. cerevisiae* and *M. jannaschii* homologs, the *Synechocystis* sp. *slr0787* bifunctional protein, and *E. coli* NadR. Asterisks indicate identical amino acids; double and single dots indicate strong and weak conserved amino acid substitutions, respectively. Gaps introduced to optimize the alignment are indicated by dashes. Boxed residues represent the novel putative consensus sequence.

was a complete match (Fig. 2), confirming that the cloned cDNA codes for NMNAT.

The hydrophobicity profile (26) of the predicted protein (Fig. 2, lower panel) suggests the existence of several potential transmembrane regions, in agreement with the observation that NMNAT is located at the inner nuclear membrane level (27). As previously reported (28), Reinhardt's method (34) for cytoplasmic/nuclear discrimination also suggests a nuclear localization. When the deduced amino acid sequence of NMNAT was examined for a number of structural motifs, we identified a single potential Asn-linked glycosylation site (<sup>36</sup>NGTG<sup>39</sup>) in the N-terminal region. To provide additional evidence that the isolated cDNA encodes NMNAT, we compared the deduced amino acid sequence with sequences of other known NMNATs.

The human enzyme was 40% identical to the yeast enzyme and 34 and 33% identical to the two putative *Caenorhabditis elegans* homologs, respectively (14). There was very little similarity with respect to the prokaryotic counterparts (12, 15, 16). In addition, we used the ClustalW program to obtain an optimized multiple sequence alignment of known NMNATs, including the NadR protein recently demonstrated to exhibit NMNAT activity (16). All proteins possess the sequence (H/T)XXH (Fig. 3), which is very similar to the motif implicated in the  $\alpha/\beta$ -phosphodiesterase activity of nucleotidyltransferases (29). Furthermore, this motif appears to be a part of the conserved sequence GXFXPX(T/H)XXH, which may represent a novel NMNAT motif. This region may constitute part of the enzyme's active center, but site-directed mutagenesis is needed to eval-



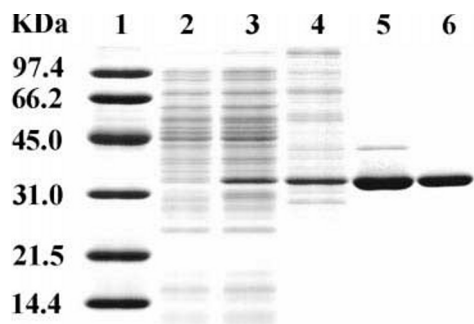


FIG. 4. **Expression and purification of recombinant human NMNAT.** A 15% polyacrylamide gel containing 0.1% SDS was stained with Coomassie Blue. Lane 1, reference proteins; lanes 2 and 3, *E. coli* BL21 containing the expression vector (10  $\mu$ g) without and with the coding sequence, respectively; lane 4, Green A fraction (10  $\mu$ g); lane 5, phenyl-Sepharose fraction (10  $\mu$ g); lane 6, 4  $\mu$ g of purified recombinant NMNAT.

uate the role of conserved sequences in NMNAT catalysis. These efforts will be augmented by ongoing x-ray diffraction studies to obtain the enzyme's three-dimensional structure.

**Expression of Human NMNAT cDNA in *E. coli* and Purification of the Recombinant Protein**—To confirm that the isolated cDNA encodes NMNAT, we developed a bacterial expression system. An 840-bp fragment containing the complete coding sequence was PCR-amplified and cloned in the polylinker region of the expression vector pT7-7 (see "Experimental Procedures"). After nucleotide sequencing of the coding insert, the resulting plasmid pT7-7-HAT was used to transform *E. coli* BL21(DE3). Transformed bacteria were induced by treatment with isopropyl- $\beta$ -D-thiogalactopyranoside to produce the recombinant enzyme. Protein extracts were prepared from the induced bacteria and assayed for NMNAT activity. Even without isopropyl- $\beta$ -D-thiogalactopyranoside, high NMNAT activity could be detected in BL21 cells transformed with the recombinant plasmid, whereas BL21 cells containing unmodified plasmid showed no detectable enzyme activity. SDS-polyacrylamide gel electrophoresis demonstrated that bacteria transformed with the recombinant plasmid contained a polypeptide of the expected size, whereas crude extracts of bacteria lacking human NMNAT-coding sequence did not (Fig. 4).

NMNAT was isolated by three chromatographic steps (Fig. 4, lanes 4–6; and Table I). The purified recombinant protein appeared as a single band with a molecular mass of 33 kDa, agreeing with the value calculated from the deduced sequence (Fig. 4, lane 6). The N-terminal sequence of the first 18 residues of the recombinant protein exactly matched the deduced sequence. The native molecular mass of the active recombinant enzyme was determined by gel filtration to be 139 kDa. These data indicate that the recombinant enzyme is an oligomer of four identical subunits, agreeing with previous experiments on the wild-type placental enzyme (13).

**Chromosomal Localization of the Human NMNAT Gene**—We were interested in investigating the chromosomal localization of the NMNAT gene to ascertain if it corresponded to the position of any known disease locus and to obtain insights regarding the genomic organization of the NMNAT locus. A fluorescent cDNA probe was used for *in situ* hybridization on metaphase chromosome spreads. The analysis showed that the NMNAT gene is located on chromosome 1p32–35 (Fig. 5). The gene for the closely related enzyme poly(ADP-ribose) polymerase is located on the same chromosome, albeit in a different region (1q41–42) (30). Genes for other enzymes in the NAD<sup>+</sup> metabolic pathway map to different chromosomes (31, 32).

**Expression of NMNAT in Human Tissues and Cancer Cell**

TABLE I  
Purification of recombinant human NMNAT

Step	Protein	Total activity	Specific activity	Yield	Purification
	mg	units	units/mg	%	-fold
Extract	146	254	1.74	100	
Green A	7.07	131	18.5	52	10.6
Phenyl-Sepharose	2.60	100	38.4	39	22.1
Superose 12	1.58	80.6	51.0	31	29.3



FIG. 5. **Chromosomal localization of the human NMNAT gene by fluorescence *in situ* hybridization.** Shown is a photograph of human metaphase chromosomes counterstained with 4,6-diamidino-2-phenylindole. Arrows point to the site of hybridization of the biotin-labeled human cDNA probe on both copies of chromosome 1 at p32–35.

**Lines**—To evaluate the distribution of NMNAT mRNA, Northern blot analyses were performed with mRNAs from various human tissues. Two messages of ~3.1 and 4.1 kilobases, respectively, were detected with variable intensity in all examined tissues. The 3.1-kilobase mRNA was considerably more abundant (Fig. 6A). The major sites of NMNAT expression were skeletal muscle, heart, liver, and kidney, whereas organs such as thymus and spleen showed a very weak signal. The widespread distribution of NMNAT in human tissues is consistent with its essential role in cellular metabolism; with no alternative biosynthetic routes for NAD synthesis, this enzyme is vitally important. However, the wide variability of NMNAT expression suggests that, in addition to its housekeeping role in pyridine metabolism, NMNAT may play a more specific role in those tissues, such as skeletal muscle, where its level is substantially higher.

Further analysis of NMNAT mRNA expression in a panel of cancer cell lines indicated that, with the exception of Burkitt's lymphoma and chronic myelogenous leukemia, the enzyme is expressed at relatively low quantities in tumor cells (Fig. 6B). This result agrees with a previous report concerning reduced NMNAT activity in cells after malignant transformation (5).

As reported above, two messages of different size were detected in all examined tissues. The library screening and the chromosomal localization suggest that both signals arise from the NMNAT locus since there were no data indicating the existence of a highly related gene that (cross-)hybridizes with

FIG. 6. **Expression of the NMNAT gene in human tissues and cancer cell lines.** A, 2  $\mu$ g of poly(A)<sup>+</sup> RNA prepared from the indicated tissues were analyzed by Northern blot hybridization with a radiolabeled probe corresponding to the coding region of human NMNAT cDNA. The positions of RNA markers are shown. Filters were subsequently hybridized with a human actin probe to ascertain the differences in RNA loading among the different samples. B, 2  $\mu$ g of poly(A)<sup>+</sup> RNA prepared from the indicated tumor cells were hybridized with the probe described for A. Filters were finally hybridized with a human actin probe. kb, kilobases.

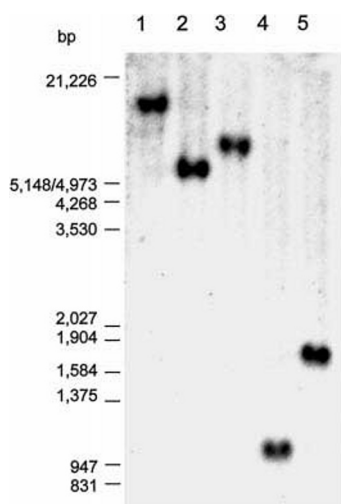
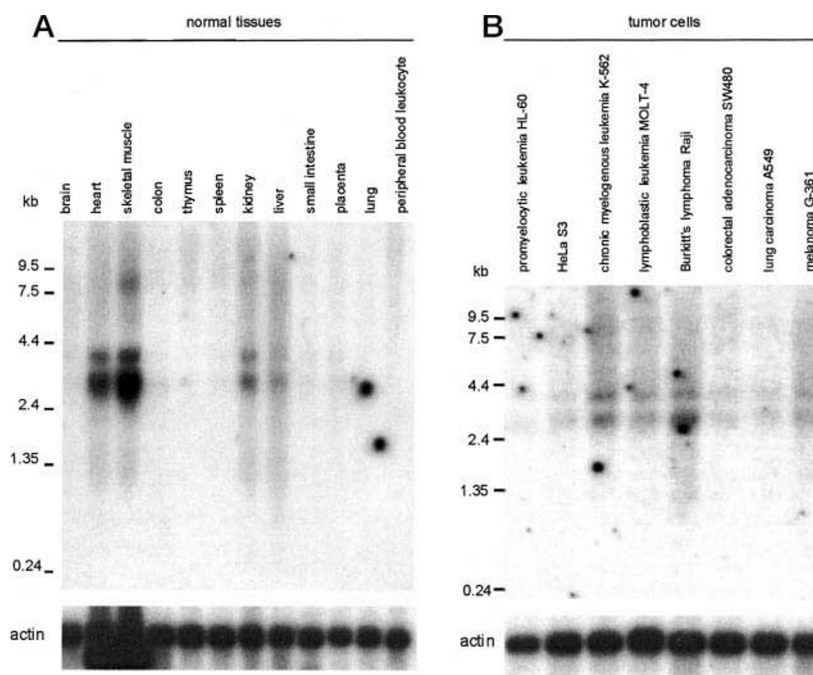


FIG. 7. **Southern blot analysis.** Human genomic DNA (10  $\mu$ g) was digested with *Apa*I, *Bam*HI, *Eco*RI, *Pst*I, or *Pvu*II. The sizes (in base pairs) of DNA markers are indicated. The fragments were separated on a 1% agarose gel, blotted, and hybridized with a 118-bp radiolabeled cDNA probe (nucleotides 800–917).

the NMNAT probe. Currently, it is not known whether the bands of different size are alternatively spliced mRNAs from the NMNAT locus or if the larger transcript represents a mRNA retaining intron sequences.

**Southern Blot Analysis**—To estimate the copy number of the NMNAT gene, genomic DNA isolated from human peripheral white blood cells was digested by one of five restriction enzymes with 6-base recognition sequences: *Apa*I, *Bam*HI, *Eco*RI, *Pst*I, or *Pvu*II. The genomic Southern blot prepared from these digests shows a single band in all lines (Fig. 7), suggesting that the NMNAT gene exists as a single copy/haploid in humans. This result agrees with the results of fluorescence *in situ* hybridization experiments, indicating that there are no other closely related loci in the human genome.

**Catalytic Properties of Recombinant Human NMNAT**—Because the functional properties of recombinant human NMNAT are of fundamental importance, we performed a detailed ki-

TABLE II  
Requirement of divalent cations for NMNAT activity  
Enzyme activity was assayed by HPLC as described under "Experimental Procedures."

Metal ion	Conc	Relative activity	$K_{app}$
	mM	%	$\mu$ M
None		0	
Mg <sup>2+</sup>	12	100	226
Mn <sup>2+</sup>	6	58	153
Co <sup>2+</sup>	1	86	161
Ni <sup>2+</sup>	1	83	173
Zn <sup>2+</sup>	0.3	63	28

TABLE III  
Kinetic parameters of purified recombinant NMNAT

The standard assay as described under "Experimental Procedures" was used with concentrations in the range of 0.02–5 mM for all substrates.  $K_m$  and  $V_{max}$  were fitted with linear regression analysis. One unit of enzyme catalyzes the synthesis of 1  $\mu$ mol of NAD<sup>+</sup>/min at 37 °C. NaMN, nicotinic acid mononucleotide.

Substrate	$K_m$	$V_{max}$	Substrate efficiency ( $V_{max}/K_m$ )
	mM	units/mg	
NMN	0.023	51	2217
NaMN	0.116	76.5	659
ATP	0.036	51	1417
dATP	0.45	15.4	34

netic characterization. The activity profile of recombinant NMNAT at different pH values using 30 mM BisTris-HCl and 30 mM Tris-HCl buffer mixtures was determined. Like other NMNATs (10–13), recombinant human NMNAT exhibited a broad pH optimum, ranging from pH 6.0 to 8.0. As observed with the enzyme purified from other sources (10–12, 15), recombinant human NMNAT absolutely required divalent cations. Optimal activity occurred in the presence of 12 mM Mg<sup>2+</sup>, but other metal ions can replace magnesium (Table II). Noteworthy is the very low  $K_{app}$  value of the enzyme for Zn<sup>2+</sup>. The results reported above seem to indicate a similarity, with respect to the cation requirement, between human NMNAT and its thermophilic counterpart, whereas the yeast recombinant enzyme exhibits maximal activity with Ni<sup>2+</sup> (14, 33). As de-

scribed previously for the native enzyme (13), the activity of recombinant human NMNAT was very depressed by several heavy metal ions, including  $\text{Hg}^{2+}$ ,  $\text{Cd}^{2+}$ ,  $\text{Cu}^{2+}$ , and  $\text{Cr}^{3+}$ , when present in the assay mixture at a concentration of 250  $\mu\text{M}$ .

Recombinant human NMNAT exhibited linear kinetics with respect to NMN and ATP; the Michaelis constants for these reactants, reported in Table III, as well as the substrate inhibition exerted by ATP, especially at low levels of NMN, are in good agreement with the catalytic properties described previously for the native enzyme (13). When deamido-NMN was used as the substrate, the reaction occurred at a comparable rate with respect to that measured in the presence of NMN; however, the higher  $K_m$  value calculated for nicotinic acid mononucleotide, with respect to NMN, suggests that, in human as well as in other eukaryotes, the amido pathway is predominant (10). Table III shows that the human enzyme can replace ATP with its deoxy form, even though with a considerably lower reaction rate, as described previously for the yeast enzyme (14).

The results reported above clearly indicate that the recombinant enzyme possesses a kinetic behavior indistinguishable from that of the native form. Therefore, the availability of the human cDNA encoding NMNAT should allow more detailed studies on the function and structure of this enzyme. In this regard, a further investigation on the specificity exhibited by recombinant human NMNAT will be helpful to expand our view of metabolic pathways that could involve NMNAT and to evaluate its functional role in human cellular homeostasis.

**Acknowledgments**—We gratefully acknowledge Prof. Mariano Rocchi (Institute of Genetics, University of Bari, Bari, Italy) for help with the chromosomal localization and Dr. Marta Menegazzi (Department of Neuroscience and Vision, Laboratory of Biological Chemistry, University of Verona, Verona, Italy) for valuable assistance in Northern blot experiments.

#### REFERENCES

- Jacobson, E. L., Shieh, W. M., and Huang, A. C. (1999) *Mol. Cell. Biochem.* **193**, 69–74
- Magni, G., Amici, A., Emanuelli, M., and Raffaelli, N. (1999) *Adv. Enzymol. Relat. Areas Mol. Biol.* **73**, 135–182
- Greenbaum, A. L., and Pinder, S. (1968) *Biochem. J.* **107**, 63–67
- Solao, P. B., and Shall, S. (1971) *Exp. Cell Res.* **69**, 295–300
- Hughes, K. T., Ladika, D., Roth, J. R., and Olivera, B. M. (1983) *J. Bacteriol.* **155**, 213–221
- Morton, R. K. (1971) *Nature* **181**, 540–542
- Emanuelli, M., Raffaelli, N., Amici, A., Balducci, E., Natalini, P., Ruggieri, S., and Magni, G. (1995) *Biochem. Pharmacol.* **49**, 575–579
- Jayaram, H. N., Pillwein, K., Lui, M. S., Faderan, M. A., and Weber, G. (1986) *Biochem. Pharmacol.* **35**, 587–593
- Boulton, S., Kyle, S., and Durkacz, B. W. (1997) *Br. J. Cancer* **76**, 845–851
- Natalini, P., Ruggieri, S., Raffaelli, N., and Magni, G. (1986) *Biochemistry* **25**, 3725–3729
- Balducci, E., Orsomando, G., Polzonetti, V., Vita, A., Emanuelli, M., Raffaelli, N., Ruggieri, S., Magni, G., and Natalini, P. (1995) *Biochem. J.* **310**, 395–400
- Raffaelli, N., Pisani, F. M., Lorenzi, T., Emanuelli, M., Amici, A., Ruggieri, S., and Magni, G. (1997) *J. Bacteriol.* **179**, 7718–7723
- Emanuelli, M., Natalini, P., Raffaelli, N., Ruggieri, S., Vita, A., and Magni, G. (1992) *Arch. Biochem. Biophys.* **298**, 29–34
- Emanuelli, M., Carnevali, F., Lorenzi, M., Raffaelli, N., Amici, A., Ruggieri, S., and Magni, G. (1999) *FEBS Lett.* **445**, 13–17
- Raffaelli, N., Lorenzi, T., Amici, A., Emanuelli, M., Ruggieri, S., and Magni, G. (1999) *J. Bacteriol.* **181**, 5509–5511
- Helman, U., Wernstedt, C., Góñez, J., and Heldin, C.-H. (1995) *Anal. Biochem.* **224**, 451–455
- Altschul, S. F., Warren, G., Webb, M., Myers, E. W., and Lipman, D. J. (1990) *J. Mol. Biol.* **215**, 403–410
- Studier, F. W., and Moffat, B. A. (1986) *J. Mol. Biol.* **189**, 435–443
- Balducci, E., Emanuelli, M., Raffaelli, N., Ruggieri, S., Amici, A., Magni, G., Orsomando, G., Polzonetti, V., and Natalini, P. (1995) *Anal. Biochem.* **228**, 64–68
- Lichter, P., Tang-Chang, C.-J., Call, K., Hermanson, G., Evans, G. A., Housman, D., and Ward, D. C. (1990) *Science* **247**, 64–69
- Southern, E. M. (1975) *J. Mol. Biol.* **98**, 503–517
- Laemmli, U. K. (1970) *Nature* **227**, 680–685
- Bradford, M. M. (1976) *Anal. Biochem.* **72**, 248–250
- Kozak, M. (1991) *J. Cell Biol.* **115**, 887–903
- Kyte, J., and Doolittle, R. F. (1982) *J. Mol. Biol.* **157**, 105–132
- Humbert, J.-P., Matter, N., Artault, J.-C., Köppler, P., and Malviya, A. N. (1996) *J. Biol. Chem.* **271**, 478–485
- Hogebom, G. H., and Schneider, W. C. (1952) *J. Biol. Chem.* **197**, 611–620
- Bork, P., Holm, L., Koonin, E. V., and Sander, C. (1995) *Proteins Struct. Funct. Genet.* **22**, 259–266
- Cherney, B. W., McBride, O. W., Chen, D. F., Alkhatib, H., Bhatia, K., Hensley, P., and Smulson, M. E. (1987) *Proc. Natl. Acad. Sci. U. S. A.* **84**, 8370–8374
- Williams, S. R., Goddard, J. M., and Martin, D. W., Jr. (1984) *Nucleic Acids Res.* **12**, 5779–5787
- Funakoshi, I., Kato, H., Horie, K., Yano, T., Hori, Y., Kobayashi, H., Inoue, T., Suzuki, H., Fukui, S., Tsukahara, M., Kajii, T., and Yamashina, I. (1992) *Arch. Biochem. Biophys.* **295**, 180–187
- Raffaelli, N., Lorenzi, T., Emanuelli, M., Amici, A., Ruggieri, S., and Magni, G. (2001) *Methods Enzymol.* **331**, in press